Chapter 4: Modeling of a demyelinated nerve and quantification of demyelination

Contents

What you do today can improve all your tomorrows.
-Ralph Marston

4.1 Introduction

The reduction of nerve conduction velocity (NCV) is a major concern for human peripheral nerve diseases such as Guillain-Barre Syndrome (GBS) and chronic inflammatory demyelinating polyneuropathy (CIDP) [1, 2]. It is caused due to the loss of myelin sheaths in axon of nerve. Measurement of reduction of myelin width is a challenging issue for clinical analysis in demyelinating polyneuropathic patients [3]. The node of Ranvier tends to disappear with demyelination and as a result the movement of ions from one side to other side of node in nerve fiber becomes slow due to non-occurring of saltatory movement. The propagation of action potential sequence (representing neuro signals) is normally analyzed by NCV signals. So, the theoretical and experimental estimation of reduction in myelin thickness requires formulation of NCV in terms of myelin thickness. Experimental validation in neurobiology is a special type of biomedical experimentation with the practice of using animal models to study and validate the pathophysiology, symptomatology and response to therapeutic inventions. The validation with the use of animal models includes theoretical formulation of an algorithm and predictive calculations of number of statistical parameters for a biological model under human environmental conditions. In this direction, a toad was used where its sciatic nerve is used as a replica for human nerve due to its neuro functional and anatomical similarities.

Snake venom especially *Naja kaouthia* (Nk) venom causes degradation of myelin sheath due to having high percentage of phospholipase A_2 (PLA_2), neurotoxins and cytotoxins [4-7]. In fact, Nk-PLA_2 belonging to lypolytic enzyme family catalyzes the hydrolysis of fatty acid esters at position 2 of 1, 2 diacyl-sn-phosphoglycerides producing lysophospholipids and free fatty acids [8]. So Nk venom is one of the strong candidates for demyelination of myelin sheath due to the presence of Nk-PLA_2. The development of toad nerve model has revolutionized the field of neuroscience especially for human peripheral clinical treatment [9-10]. Moreover, the membrane transport and activity of neurotransmitter are better examined on isolated toad nerve having bundle of axons [11-12].

Clinical monitoring of the demyelinating diseases requires rapid and non-invasive quantification of demyelination. In this chapter, the formulation of NCV in

terms of demyelination considering electric circuit model of a nerve having bundle of axons for its quantification from NCV measurements has been validated using a toad model in this section. A sciatic nerve isolated from toad has been demyelinated using crude Nk venom and this demonstration also shows the effect of PLA_2 and three finger toxin (3FTx) from Nk-venom on peripheral nerve.

4.2 Modeling of a demyelinated nerve

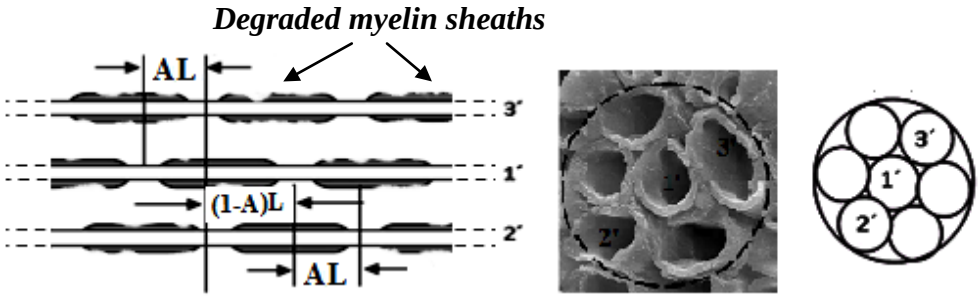

(a) (b) (c)

Figure 4.1: (a) A bundle of axons in a demyelinated nerve fiber with degraded myelin sheath, (b) image representing a bundle of axons in a demyelinated nerve obtained from scanning electron microscope (SEM) and (c) schematic representation of bundle of axons corresponding to SEM image.

Fig-4.1 represents a demyelinated nerve consisting of a bundle of axons, where the myelin sheath is degraded non-uniformly. The alignment of nodes in the axon is defined by an alignment parameter A and L is the internodal length of the axon (as discussed in chapter 3).

A theory of electrical circuit model of demyelinated nerve has been rigorously reviewed and reported by many authors [13-15] to analyze the nerve fiber of human body. The process of demyelination decreases the amount of myelin (as shown in Fig-4.1), thereby affecting the axoplasmic resistance, periaxonal resistance and peranodal seal resistance of the nerve [16]. These lead the reduction of the internal resistance of the axon, contributing the decrease of total resistance whereas the reduction of myelin resistance affecting the external resistance. On the other hand, capacitance and the ionic

conductance of the respective ions namely sodium ion, fast potassium, slow potassium and the other ions (leakage) increases with the increase in demyelination. In this section, a mathematical model of demyelinated nerve incorporation with a demyelinating factor (γ), as a function of myelin thickness which is defined as the ratio of change in myelin thickness due to demyelination to the original myelin thickness of a normal nerve and is formulated to describe nerve conduction properties in the peripheral nerves of demyelinating patients.

4.2.1 Electric circuit model

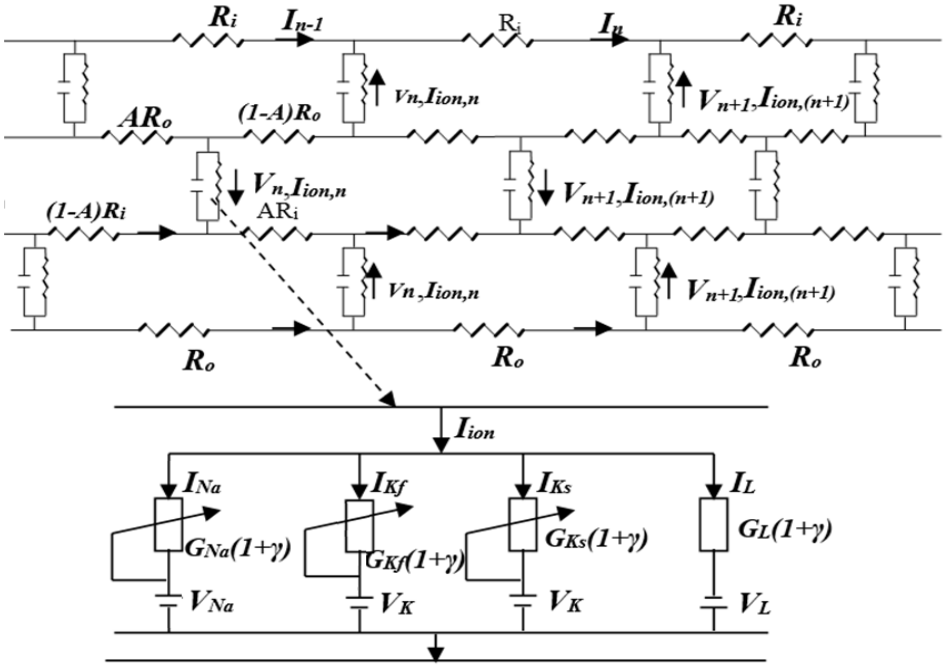

Figure 4.2: Electric circuit model of a demyelinated nerve.

Fig-4.2 represents an electric circuit model of a peripheral nerve with reduction of myelin thickness consisting of an internal resistance of $R_i=R_i(1-\gamma)$ (where R_i is the internal resistance of normal myelinated nerve, external resistance), $R_o=R_o(1-\gamma)$ (where R_o is the external resistance of normal myelinated nerve), membrane capacitance $C(1+\gamma)$, (where C is capacitance of normal myelinated nerve contributed by membrane, nodal and axolemmal capacitance) and ionic conductance $G_{Na}(1+\gamma)$, $G_{Kf}(1+\gamma)$, $G_{Ks}(1+\gamma)$ and $G_L(1+\gamma)$ (where $G_{Na,}$ G_{Kf}, G_{Ks} and G_L are ionic conductance of sodium ions, fast potassium and slow potassium and leakage ions such as chlorine and calcium ions, respectively for normal myelinated nerve). Hodgkin-Huxley (H-H) electrical circuit

model for giant nerve is modified considering bundle of axons as shown in Fig-4.1 and Fig-4.2. The ephaptic interactions between action potential impulses of parallel axons in a bundle is demonstrated to describe NoR misalignment among axons (Fig-4.1). The currents responsible due to flow of sodium, fast potassium, slow potassium and other ions known as the leakage currents are denoted by I_{Na}, I_{Kf}, I_{Ks} and I_L and can be written in terms of conductance and potential with cubic polynomial function approximation and considering resting potential zero at equilibrium incorporation with a demyelinating factor γ as-

$$I_{Na} = \left(\frac{G_{Na}(1+\gamma)}{V_{Na}(V_{Na} - V_{th}^{Na})}\right) V_n (V_n - V_{th}^{Na})(V_n - V_{Na})$$

$$I_{Kf} = \left(\frac{G_{Kf}(1+\gamma)}{V_K(V_K - V_{th}^{Kf})}\right) V_n (V_n - V_{th}^{Kf})(V_n - V_K)$$

$$I_{Ks} = \left(\frac{G_{Ks}(1+\gamma)}{V_K(V_K - V_{th}^{Ks})}\right) V_n (V_n - V_{th}^{Ks})(V_n - V_K)$$

$$I_L = \left(\frac{G_L(1+\gamma)}{V_L(V_{Na} - V_{th}^{L})}\right) V_n (V_n - V_{th}^{L})(V_n - V_L) \quad (4.1)$$

Where V_n is the voltage at node *n*. V_{th}^{Na}, V_{th}^{Kf}, V_{th}^{Ks} and V_{th}^{L} are the threshold voltages of sodium, fast potassium, slow potassium and leakage component respectively, at which sodium, fast potassium, slow potassium and leakage current begins to flow into an active node. V_{Na}, V_K and V_L are Nernst (diffusion) potentials at which the ionic currents for sodium, fast potassium, slow potassium and leakage current respectively in the demyelinated nerve.

4.2.2 Formulation of NCV

In this section nerve conduction values for varying demyelination factors have been estimated by using electrical circuit model as shown in Fig-4.2. Applying Kirchoff's voltage law, the current at node *n-1* and node n is written as

$$I_{n-1} = (V_{n-1} - V_n)/\{(R_i + R_o)(1-\gamma)\} \tag{4.2}$$

$$I_n = (V_n - V_{n+1})/\{(R_i + R_o)(1-\gamma)\} \tag{4.3}$$

From Kirchoff's current law, the current can be written as

$$I_{n-1} - I_n = C(1+\gamma)\frac{\partial V_n}{\partial t} + I_{ion,n} \tag{4.5}$$

Using equation (4.2), (4.3) and (4.4), equation (4.5) becomes

$$[(V_{n-1} - V_n)/\{(R_i + R_o)(1-\gamma)\}] - [(V_n - V_{n+1})/\{(R_i + R_o)(1-\gamma)\}] = C(1+\gamma)\frac{\partial V_n}{\partial t} + I_{ion,n} \tag{4.6}$$

The total resistance *R* is reduced to *R(1-γ)* due to demyelination in a demyelinated nerve. Thus, equation (4.6) becomes

$$1/\{R(1-\gamma)\}\ [V_{n-1} - 2V_n + V_{n+1}] = C(1+\gamma)\frac{\partial V_n}{\partial t} + I_{ion,n} \tag{4.7}$$

Using equations (4.1), equation (4.7) can be written as

$$\{1/R(1-\gamma)\}[V_{n-1} - 2V_n + V_{n+1}] = C(1+\gamma)\frac{\partial V_n}{\partial t}$$

$$+\left(\frac{G_{Na}(1+\gamma)}{V_{Na}(V_{Na} - V_{th}^{Na})}\right)V_n(V_n - V_{th}^{Na})(V_n - V_{Na})$$

$$+\left(\frac{G_{Kf}(1+\gamma)}{V_K(V_K - V_{th}^{Kf})}\right)V_n(V_n - V_{th}^{Kf})(V_n - V_K)$$

$$+\left(\frac{G_{Ks}(1+\gamma)}{V_K(V_K - V_{th}^{Ks})}\right)V_n(V_n - V_{th}^{Ks})(V_n - V_K)$$

$$+(\frac{G_L(1+\gamma)}{V_L(V_{Na}-V_{th}^L)})V_n(V_n-V_{th}^L)(V_n-V_L) \tag{4.8}$$

Replacing $1/RC(1-\gamma^2)$ by D, where D is a diffusion constant in squared centimeters per second^2 in equation (4.8), then, in this formulation, the dynamic equation becomes

$$D[V_{n-1}-2V_n+V_{n+1}]=\frac{\partial V_n}{\partial t}$$

$$+\{1/C(1+\gamma)\}[(\frac{G_{Na}(1+\gamma)}{V_{Na}(V_{Na}-V_{th}^{Na})})V_n(V_n-V_{th}^{Na})(V_n-V_{Na})$$

$$+(\frac{G_{Kf}(1+\gamma)}{V_K(V_K-V_{th}^{Kf})})V_n(V_n-V_{th}^{Kf})(V_n-V_K)$$

$$+(\frac{G_{Ks}(1+\gamma)}{V_K(V_K-V_{th}^{Ks})})V_n(V_n-V_{th}^{Ks})(V_n-V_K)$$

$$+(\frac{G_L(1+\gamma)}{V_L(V_{Na}-V_{th}^L)})V_n(V_n-V_{th}^L)(V_n-V_L)] \tag{4.9}$$

The equation (4.9) represents a discrete reaction diffusion equation of myelinated nerve. Equation (4.9) can be written in continuum limit as partial differential equation which is given below

$$D\frac{\partial^2 t}{\partial x^2}-\frac{\partial V_n}{\partial t}=\{1/C(1+\gamma)\}[(\frac{G_{Na}(1+\gamma)}{V_{Na}(V_{Na}-V_{th}^{Na})})V_n(V_n-V_{th}^{Na})(V_n-V_{Na})$$

$$+(\frac{G_{Kf}(1+\gamma)}{V_K(V_K-V_{th}^{Kf})})V_n(V_n-V_{th}^{Kf})(V_n-V_K)$$

$$+\left(\frac{G_{Ks}(1+\gamma)}{V_K(V_K-V_{th}^{Ks})}\right)V_n(V_n-V_{th}^{Ks})(V_n-V_K)$$

$$+\left(\frac{G_L(1+\gamma)}{V_L(V_{Na}-V_{th}^{L})}\right)V_n(V_n-V_{th}^{L})(V_n-V_L)] \tag{4.10}$$

In the bundle of demyelinated nerves, total resistance, $R=R_i\,(1-\gamma)+R_o(1-\gamma)A(N-1)$ and coupling constant, α (as shown in sub section 3.3.2 of chapter 3) is given by

$$\alpha=\frac{R_i(1-\gamma)}{R_i(1-\gamma)+R_O(1-\gamma)A(N-1)} \tag{4.11}$$

Therefore, the equivalent resistance in the bundle becomes

$$R=\frac{R_O(1-\gamma)A(N-1)}{(1-\alpha)} \tag{4.12}$$

Thus, the NCV in the demyelinated nerve using traveling wave solutions of equation with leading edge approximation (as discussed in the previous chapter) in terms of coupling constant and alignment factor in a bundle of axons in the nerve fiber is given by-

$$v_C=\sqrt{\frac{G_{Na}(1+\gamma)(1-\alpha)}{R_O(1-\gamma)A(N-1)\{C(1+\gamma)\}^2}}\frac{V_{Na}-2V_{th}^{Na}}{\sqrt{2V_{Na}}}(1-\gamma)$$

$$+\sqrt{\frac{G_{Kf}(1+\gamma)(1-\alpha)}{R_O(1-\gamma)A(N-1)\{C(1+\gamma)\}^2}}\frac{V_K-2V_{th}^{Kf}}{\sqrt{2V_K}}(1-\gamma)$$

$$+\sqrt{\frac{G_{Ks}(1+\gamma)(1-\alpha)}{R_O(1-\gamma)A(N-1)\{C(1+\gamma)\}^2}}\frac{V_K-2V_{th}^{Ks}}{\sqrt{2V_K}}(1-\gamma)$$

$$+\sqrt{\frac{G_L(1+\gamma)(1-\alpha)}{R_O(1-\gamma)A(N-1)\{C(1+\gamma)\}^2}}\frac{V_L-2V_{th}^L}{\sqrt{2V_L}}(1-\gamma) \tag{4.13}$$

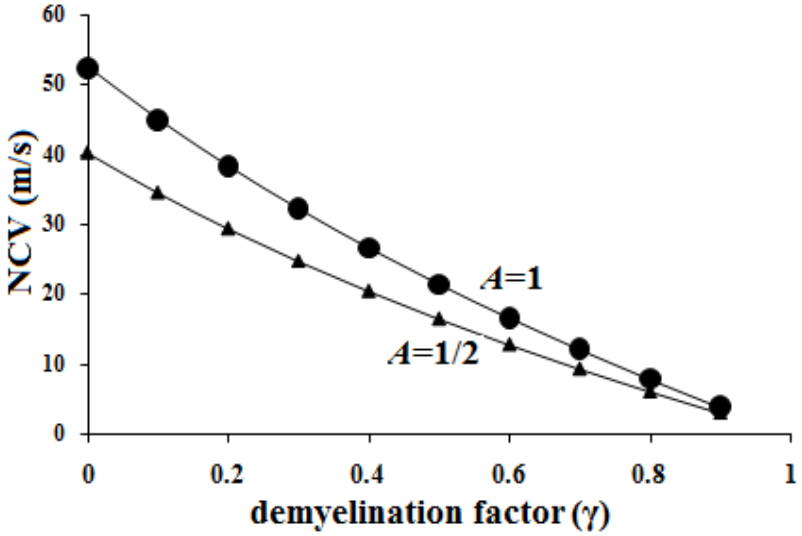

Figure 4.3: Estimation of NCV in terms of demyelination factor with alignment parameter *A*.

Fig-4.3 shows NCV versus demyelination estimated by using equation (4.13) and considering standard parameters shown in Table-3.1 (chapter 3). As observed in case of myelinated nerves (discussed in chapter 3), the aligned demyelinated nerves posses' higher value of NCV than that of a demyelinated nerve with bundle of misaligned axons.

4.3 Demyelination in a toad nerve model

The formulation of NCV in terms of demyelination considering electric circuit model of a nerve having bundle of axons for its quantification from NCV measurements is validated using a toad nerve model in this section. A sciatic nerve isolated from toad is demyelinated using crude Nk venom and this demonstration also shows the effect of PLA_2 and 3FTx from Nk-venom on peripheral nerve.

4.3.1 Materials and methods

Some of the materials along with the chemicals including Ringers solution, Chloroform and ethanol for cleaning purpose are already mentioned in chapter 3. This section also deals with the various steps applied to conclude the demyelination experiment on toad.

4.3.1.1 Animals

Common Asian toads (*Duttaphrynus melanostictus*) which are found in the lawns and gardens of the university campus are collected and used for neurotoxicity studies. Sciatic nerves of the collected toads are isolated and used for validation of NCV and calibrating compound action potential (CAP) recordings. The experiments on toads are performed 5-6 times and standard deviation (SD) is estimated to minimize the percentage of error during the experiments. For performing the experiments, 24 toads of same age (~1-2 months) are taken for validation of demyelination measurements from nerve conduction velocity and divided into four groups (A, B, C and D). The sciatic nerves of toads of group A is not treated with crude venom whereas the sciatic nerves of B,C and D groups are treated with Nk venoms of 0.1 μg/ml, 1μg/ml and 10μg/ml respectively.

4.3.1.2 Collection of snake venom

Crude venom, Nk-PLA_2 and 3Ftx from Nk of North East India are managed from the Department of Molecular Biology and Biotechnology, Tezpur University, Napaam, Tezpur, Assam, India. The permission for milking of snakes from Assam is obtained from Principal Chief Conservator of Forest (Wild Life) and Chief Wild Life Warden of Assam, India (WL/FG.27/tissue Collection/09 dated 07/10/2011).

4.3.1.3 Determination of Protein content

The total protein concentration of crude Nk and purified toxin is determined by Lowry's method [17]. The basic principle behind this method is that at 660 nm wavelength, the phenolic group of amino acid (tyrosine and tryptophan residue) in the protein produced blue purple color complex with Folin-Ciocalteau reagent which consists of sodium tungstste molybdate and phosphate. Bovine Serum Albumin (BSA) solution is used as a standard protein for the estimation of total protein by Lowry's method because of its low cost, high purity and easy availability. The Lowry's method is pH sensitive and its working range is maintained at 10-10.5. This narrow range of pH has been the major disadvantage of this method within which it is very accurate. However, for small volumes of sample, it has little or no effect on the reaction mixture [17, 18].

4.3.1.4 Venom enzyme assay

The toxicity of snake venom relies on the qualitative and quantitative distribution of a variety of enzymes, non-enzymatic polypeptide toxins and non-toxic proteins in the venom [19]. Caseinolytic, plasma protease, PLA_2, adenosine monophosphatase, adenosine triphosphatase and acetylcholinesterase activities are the possession of used Nk venom. Total protein content of Nk venom was determined according to Lowry's method using BSA as standard [17]. Egg phoshotidylcholine as a substrate is used to assay Phospholipase A_2 activity by free fatty acid liberation [20]. The other enzymatic activities are performed according to the assays performed by previous authors [19, 21]. A semi quantitative test is performed for L–Amino acid oxidase but it was found absent in the venom.

Table 4.1: Enzymes and their composition in *Naja Kaouthia* [19]

Enzyme parameters	***Enzyme activity (unit/mg protein)***
Caseien	5.2 ± 0.4
Phospholipase A_2	110 ± 7.0
Adenosine monophosphatase	118 ± 9.0
Adenosine triphosphatase	100 ± 5.5
Acetyl cholinesterase	26 ± 1.5

4.3.1.5 Partial purification of fraction containing Phospholipase A_2 (PLA_2) and three finger toxin (3FTx)

Crude venom is subjected to single step fractionation on reversed phase-High performance Liquid Chromatography (RP-HPLC) using symmetry C18 column (5µ, 4.6x250 mm, 300Å) (Waters, USA). Fractionation is carried out in a linear gradient of buffer B (80% acetonitile (ACN) containing 0.1% Trifluoroacetic acid (TFA)) in a pre-equilibrated column with buffer A (0.1% TFA in milli Q water) on a High performance Liquid Chromatography (HPLC) system (Waters, USA). Eluted protein peaks are monitored at 215 and 280 nm and collected manually. Considering the retention time of the protein peaks likely to contain PLA_2 and 3FTxs are isolated.

4.3.1.6 Phospholipase A_2 activity assay

PLA_2 activities of the crude venom as well as the fractionated peaks were determined according to Doley and Mukherjee [22] using egg yolk as a substrate. One unit of PLA_2 activity is defined as the amount of protein which produces a decrease in 0.01 absorbance at 740nm within 10mins.

4.3.1.7 Recording of CAPs and estimation of NCV from the prepared sciatic nerves

The procedure for recording the CAPs and determination of NCV from the neuro signals generated by the sciatic nerve using AD Instruments remains the same as discussed in the previous chapter (sub section 3.4.2.2 of chapter 3). The venom treated nerves are mounted separately on the nerve chamber to collect the nerve conduction signals to their respective venom concentrations. A frequency of 1Hz for duration of 0.1ms is applied on the treated sciatic nerves of toad to determine the CAP. Nerve only treated with Ringer's solution is considered as control. The nerves are also treated with purified Nk-PLA_2 and 3Ftx to study the neurotoxic effect from the signals of the treated nerve. The experiments are performed six times and standard deviation (SD) is estimated to minimize the percentage of error as per standard method [23]. Finally, the NCV is estimated using data collected from the signal and the distance-latency formula.

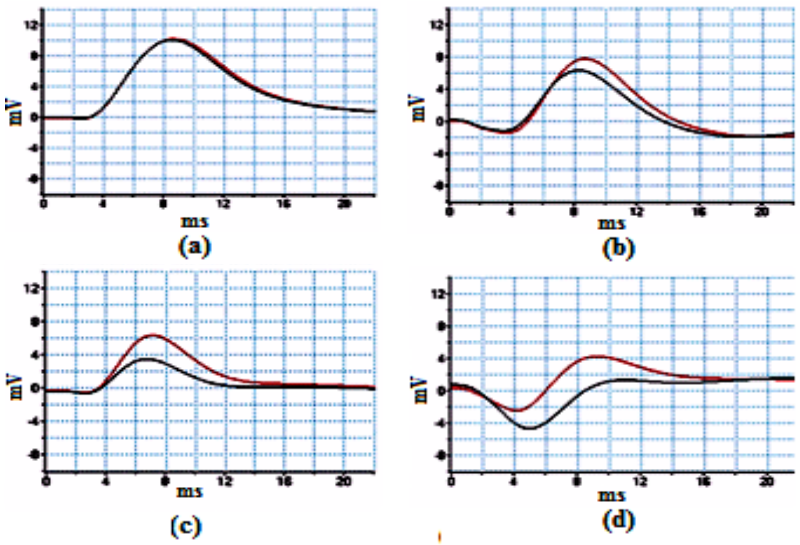

Figure 4.4: Electric neuro signals of (a) control, and nerves treated with (b) 0.1µg/ml, (c) 1.0µg/ml and (d) 10µg/ml of crude venom concentrations respectively.

4.3.1.8 Scanning Electron Microscope (SEM) imaging

Sciatic nerves are subjected for SEM analysis to check the effect of crude venom on morphology of the isolated nerve as shown in Fig-4.5. Sciatic nerve preparations are incubated for 15mins before fixation is performed on the prepared isolated sciatic nerves of toad. Firstly, the nerves are subjected to primary fixation using 2.5% gluteraldehyde for 4hr followed by secondary fixation using 1% OsO_4 (Osmium tetroxide) for 4hr for better penetration. Cross section of sciatic nerve was made by slicing at a length of 10mm using glass cutter in a microtome for maintaining uniformity. The sliced nerve segments are further observed under SEM for the structural change. The thickness of myelin in the isolated nerves considering 6-7 nerves in a bundle is quantified with the use of measuring scale installed in the SEM.

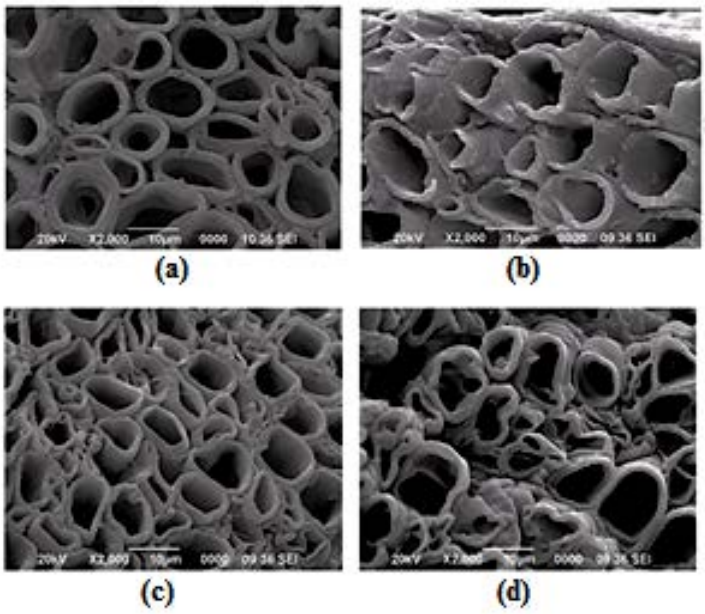

Figure 4.5: SEM images of (a) control, and nerves treated with (b) 0.1µg/ml, (c) 1.0µg/ml and (d) 10µg/ml of crude venom concentrations respectively.

4.4 Results

For experimental estimation of demyelination, sciatic nerves are isolated from toad and its storage was made in Ringer's solution. During experiments on nerve conduction by using AD instruments, the sciatic nerves are kept moist in nerve chamber using Ringer's

solution. The reduction of myelin thickness (i.e., demyelination) with increase of crude venom concentration is confirmed by SEM images in Fig-4.5.

Table 4.2: Relation between myelin thickness and NCV with different concentration of crude Nk venom

Parameters	**Toad sciatic nerve treatment with crude Nk venom**			
	0µg/ml	**0.1µg/ml**	**1µg/ml**	**10µg/ml**
Myelin thickness (µm)	1.79±0.05	1.22±0.15	1.00±0.9	0.91±0.08
NCV (m/s)	32.90±0.21	21.95±0.99	18.33±1.2	14.28±0.85

SEM image of normal sciatic nerves with myelin thickness of 1.79±0.05µm possess a NCV of 32.90±0.21m/s. As the nerve is treated with an increase dose of crude venom concentration from 0.1µg/ml to 10µg/ml, the reduction in NCV also increases. The reduced NCV in nerves demyelinated with 0.1µg/ml, 1.0µg/ml and 10µg/ml of crude venom are 21.95±0.99m/s, 18±0.33m/s and 14.28±0.85m/s with demyelinated myelin thickness of 1.22±0.15µm, 1.00±0.9µm and 0.91±0.08µm respectively as obtained from Fig-4.4, Fig-4.5 and Table 4.2. The propagation of action potential is estimated experimentally by applying stimuli on sciatic nerves treated with different crude Nk venom concentration as shown in Fig-4.4. The nerve conduction signals obtained from proximal and distal action potential nerve treated with 0.1µg/ml, 1.0µg/ml and 10µg/ml crude Nk venom concentration shows reduction of nerve conduction velocity (NCV) due to demyelination of axons in the nerve (Table-4.3). The neuro signals recorded from demyelinated nerves treated with 0.1µg/ml, 1µg/ml and 10µg/ml of Nk venom, the NCV are found to be 26.62±0.58m/s, 18.25±0.25m/s and 15.87±0.15m/s for their corresponding venom concentrations as shown in Table-5.2. The change in pattern of NCV in the experiment where nerves treated with crude venom and purified PLA_2 represented by black dots and black triangles as shown in Fig-4.6 finds a similarity curve with the change in NCV (represented by straight line) obtained theoretically from the formulation (equation-4.11) using MATLAB and these values of NCV are used to predict the amount of demyelination as shown in the curve of the figure. Estimation of demyelination from NCV formulation will avoid the invasive difficulties of SEM imaging and nerve biopsy. The rate of increase of demyelination

(ΔD) with crude venom concentration is very fast up to 1μg/ml and it becomes saturated after that (inset of Fig-4.6).

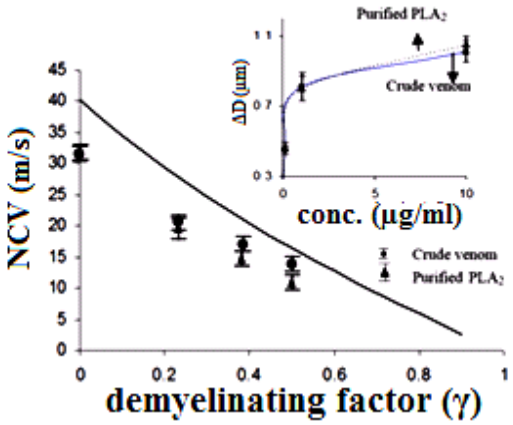

Figure 4.6: A graphical representation of NCV versus demyelinating factor with an inset of degree of demyelination versus crude venom concentration.

Table 4.3: Estimation of NCV for various concentrations of Nk crude venom

Estimation of NCV (m/s)							
Concentration of crude venom	**No. of observations**						**S.D**
	I	**II**	**III**	**IV**	**V**	**VI**	
0.1μg/ml	26.32	26.65	26.17	25.99	27.49	27.09	26.62±0.58
1μg/ml	18.02	18.43	18.60	18.13	18.11	18.21	18.25±0.22
10μg/ml	16.09	15.97	15.93	15.76	15.72	15.77	15.87±0.15

As seen in Fig-4.7, Nk-PLA_2 present in crude venom is mainly responsible for demyelination as per the following reaction of Nk-PLA_2 with phospholipase of myelin.

$$\text{Nk-PLA}_2 + \text{Myelin} \xrightarrow[\text{Ca}^{2++}\text{ ion as cofactor}]{\text{Hydrolysis}} \text{Lysophospholipids + free fatty acids}$$

The rate of reaction increases with increase of Nk-PLA_2 molecules (as Nk-PLA_2 concentration increase of crude venom concentration) and as a result more demyelination increases with increase in concentration of Nk-PLA_2 (Fig-4.7). γ was

estimated by calculating the ratio of change in myelin thickness due to demyelination to the actual amount of myelin thickness of the nerve and the experiment was performed for six times with normal nerves and nerves treated with 0.1µg/ml, 1.0µg/ml and 10µg/ml of crude venom and Nk-PLA_2 respectively (as shown in Table-4.2).

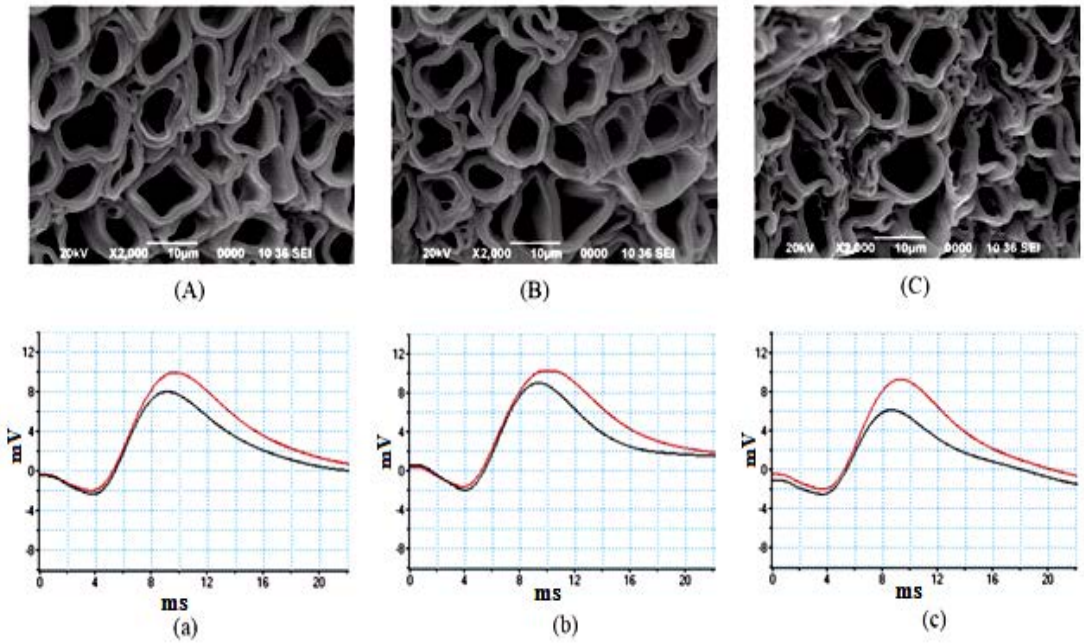

Figure 4.7: Effect of purified Nk-PLA_2 with different concentration on sciatic nerves of toad and their nerve conduction signals (proximal and distal action potential) with corresponding SEM images of their sciatic nerves.

Table 4.4: Estimation of NCV for various concentrations of purified Nk-PLA_2

Estimation of NCV (m/s)							
Concentration of purified Nk-PLA_2	**No. of observations**						**S.D**
	I	**II**	**III**	**IV**	**V**	**VI**	
0.1µg/ml	25.12	25.06	25.32	25.99	26.19	26.03	25.62±0.81
1µg/ml	16.92	17.13	17.06	16.99	17.21	17.27	17.10±0.13
10µg/ml	15.39	14.91	14.45	13.98	14.02	14.00	14.46±0.58

The nerve conduction experiment of Nk-PLA_2 (purified from Nk crude venom) treated sciatic nerves shows reduction of NCV due to demyelination in which the

variation of demyelination thickness (ΔD) with Nk-PLA_2 concentration for Nk-PLA_2 treated nerve is almost close to that of crude venom treated nerve proving major contribution of demyelination by Nk-PLA_2. The reduction of NCV affected by purified Nk-PLA_2 is found to be 25.62±0.81m/s, 17.10±0.13m/s and 14.46±0.58m/s for 0.1µg/ml, 1.0µg/ml and 10µg/ml of Nk-PLA_2 respectively as shown in Table-4.4.

Table 4.5: Demyelinating factor (γ) of a normal nerve and nerves treated with three different concentrations of crude venom and Nk-PLA_2

Sample	Demyelinating factor (γ)						
	Experiment	I	II	III	IV	V	VI
Normal Nerve		0	0	0	0	0	0
Crude venom	0.1µg/ml	0.3271	0.3220	0.3184	0.3111	0.3186	0.3128
	1.0µg/ml	0.4406	0.4406	0.4469	0.4333	0.4341	0.4413
	10µg/ml	0.4972	0.4972	0.4972	0.4889	0.4890	0.4810
Nk-PLA_2	0.1µg/ml	0.2203	0.2147	0.2179	0.2167	0.2198	0.2179
	1.0µg/ml	0.3785	0.3785	0.3743	0.3667	0.3681	0.3743
	10µg/ml	0.5141	0.5141	0.5028	0.4944	0.4945	0.4972

4.4.1 Reduction of amplitude of NC signal

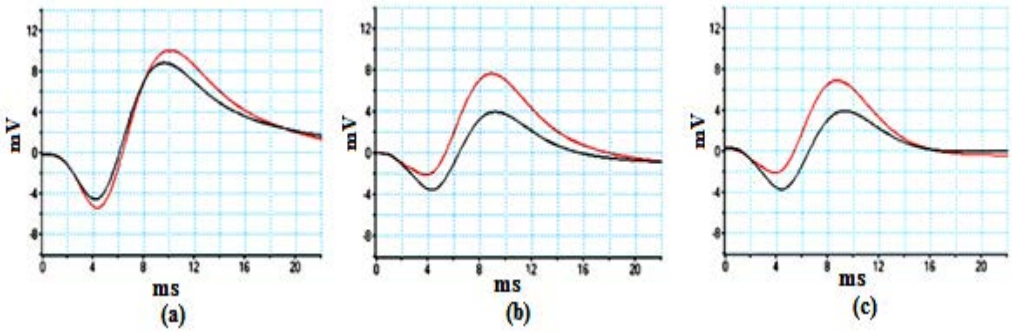

Figure 4.8: Effect of purified 3Ftx with different concentration on nerve conduction signals.

The Nerve conduction signals in Fig-4.8 shows decrease of amplitude of wave due to both Na^+ and K^+ channel blocking in crude venom treated toad nerve. The weak 3FTx

which constitutes a major percentage of cobra venom is mainly responsible for channel blockade activity in a nerve [24, 25]. 3FT-neurotoxin binds the neural Ach receptors (nAchR) causing blocking of transmission of both Na^+ and K^+ ions through the ion gated channels as shown in Fig-4.9. Fig-4.9(a) shows transportation of Na^+ into cell through cell membrane and K^+ transportation leaving from cell through membrane and provides saltatory movement of the nerve impulse (action potential) in a normal nerve. 3FTx blocks the Na+ and K+ channel by binding with AchR resulting in reduction of AP (as shown in Fig-4.9(b) and Table-4.5). The blockade increases with increase of crude venom concentration (as shown in Fig-4.9(c)-(d)). The nerve conduction experiments of 3FT-neurotoxin (purified from crude venom) treated nerve confirms reduction of action potential due to blocking of channel. There is no change of value of latency between peak of proximal and peak of distal action potential even with increase of 3FTx concentration proving no reduction of myelin thickness of sciatic nerve treated with 3FTx and it is confirmed from SEM image. The percentage of proximal CAP amplitude reduction for 0.1µg/ml, 1.0µg/ml and 10µg/ml of 3FTx are ~15%, ~16% and ~40% respectively whereas the percentage of reduced distal CAP amplitude are ~20%, ~27% and ~60% as shown in Table-4.5.

Table 4.6: Estimation of AP in nerves treated with 3FTx

No. of observations	Estimation of AP (mV) for concentrations of 3FTx					
	0.1µg/ml		1µg/ml		10µg/ml	
	Distal AP	Proximal AP	Distal AP	Proximal AP	Distal AP	Proximal AP
I	8.3	10	8.0	9.3	3.8	7.2
II	8.2	10.1	7.9	9.2	3.9	7.3
III	8.2	10.2	8.0	9.2	3.9	7.3
IV	8.1	10.2	8.0	9.3	3.6	7.1
V	8.2	10.0	7.9	9.2	3.7	7.0
VI	8	10.3	7.8	9.1	3.7	7.1
S. D	8.2±0.10	10.1±0.12	7.9±0.08	10.05±0.10	3.8±0.12	7.2±0.12

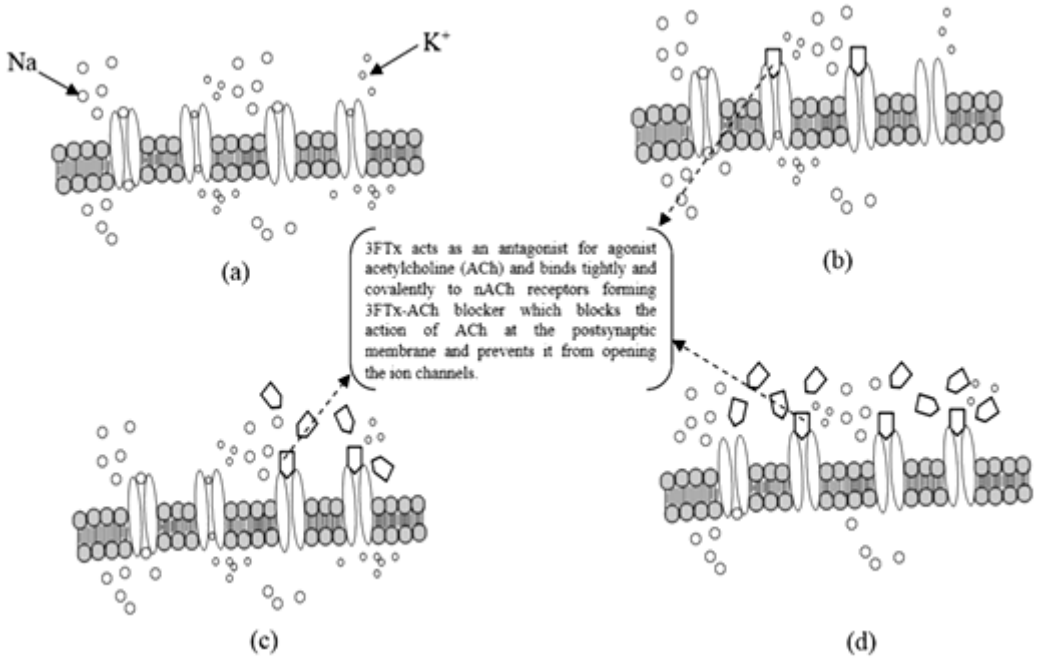

Figure 4.9: Mechanism of channel blocking in cell membrane.

4.5 Discussion

Although the experiments are performed on sciatic nerve isolated from toad the findings open a non-invasive clinical way to quantify demyelination of a peripheral nerve from NCV measurements. The observation shown here is emerging experimental evidences for demyelination and channel blockade using Nk crude venom. The proposed electric circuit model for a nerve consisting of six axons matches with experimental results of demyelination by using Nk crude venom. The results provide demyelination analysis of different critical neuro-diseases such as CIDP, GBS etc. Although the experiments are limited to peripheral sciatic nerve, the model may also quantify demyelination of central nervous system (CNS) including motor nerve from nerve conduction velocity. So, future studies are required to determine the role of crude venom in CNS demyelination. The result may extend to support non-invasive clinical analysis of CNS demyelinating diseases like multiple sclerosis, Alzheimer's disease, Epilepsy, etc. In the proposed works, channel blocking in sciatic nerve were demonstrated using 3FTx weak neurotoxin (Fig-4.9). It leads a way to quantify Na^+ and K^+ channel blocking, due to the binding of 3FTx with nAChR.

The theoretical curve of NCV versus demyelination factor (Fig-4.6) validated with nerve conduction experiments, establish a hypothesis to quantify demyelination in the patients and the demyelination of nerve is obtained from known NCV using demyelination factor as shown in the curve. This hypothesis may help the medical experts to estimate the quantity of demyelination from the range of NCV of the patients.

4.6 Conclusions

The reduction of NCV is estimated theoretically from the electric circuit model of a demyelinated nerve consisting of a bundle of demyelinated axons. The validation experiments are performed on toad nerve model where its sciatic nerves are demyelinated using Nk crude venom, Nk-PLA_2 and 3FTx. The neuro signals recorded from demyelinated nerves treated with 0.1µg/ml, 1µg/ml and 10µg/ml of Nk venom, the percentage of reduction in NCV is found to be ~20%, ~45% and ~52% for their corresponding venom concentrations. Similarly, for nerve treated with Nk-PLA_2, the percentage of reduction of NCV is ~22% for 0.1µg/ml, ~49% for 1.0µg/ml and ~56% for 10µg/ml of purified Nk-PLA_2 respectively. The amplitudes of both proximal and distal CAP decreases due to the presence of more number of channel blocking as the sciatic nerve of toads are treated with an increase dose of 3FTx. The percentage of proximal CAP amplitude reduction for 0.1µg/ml, 1.0µg/ml and 10µg/ml of 3FTx are ~15%, ~16% and ~40% respectively whereas the percentage of reduced distal CAP amplitude are ~20%, ~27% and ~60%.

Bibliography

[1] Kuwabara, S. Guillain-Barre Syndrome. *Current Neurology and Neuroscience Reports*, 7(1):57-62, 2007.

[2] Stephanova, D. L., Daskalova, M. S., and Alexandrov, A. S. Differences in membrane properties in simulated case of demyelinating neuropathies, intermodal focal demyelination with conduction block. *Journal of Biological Physics*, 32:129-144, 2006.

[3] Toothaker, T. B. & Brannagan, T. H. Chronic inflammatory demyelinating polyneuropathies: current treatment strategies. *Current Neurology and Neuroscience Reports*, 7 (1):63-70, 2007.

[4] Mukherjee, A. K. Phospholipase A2-interacting weak neurotoxins from venom of monocled cobra Naja kaouthia display cell-specific cytotoxicity. *Toxicon*, 51:1538-1543, 2008.

[5] Ogay, A. Y., Rzhevsky, D. I., Murashev, A. N., Tsetlin, V. I., & Utkin, Y, N. Weak neurotoxin from *Naja kaouthia* cobra venom affects haemodynamic regulation by acting on acetylcholine receptors. *Toxicon*, 45:93-99, 2005.

[6] Mukherjee, A. K. Correlation between the phospholipids domains of the target cell membrane and the extent of *Naja Kaouthia* PLA_2-induced membrane damage: Evidence of distinct catalytic and cytotoxic sites in PLA_2 molecules. *Biochimica et Biophysica Acta*, 1770(2):187-195, 2007.

[7] Kini, R. M. Excitement ahead: structure, function and mechanism of snake venom phospholipase A_2 enzyme. *Toxicon*, 42:827-840, 2003.

[8] Kini, R. M. Evolution of three-finger toxins - A versatile mini protein scaffold. *Acta Chimica Slovenica*, 58:693-701, 2011.

[9] Nylander, A. and Hafler, D. A. Multiple sclerosis. *Journal of Clinical Investigation*, 122:1180-1188, 2012.

[10] Yegin, A., Akbas, S. H., Ozben, T., and Korgun, D. K. Secretory phospholipase A_2 and phospholipids in neural membranes in an experimental epilepsy model. *Acta Neurologica Scandinavica*, 106(5):258-262, 2002.

[11] Steinbach, J. H. and Stevens, C. F. Neuromuscular Transmisión. In Llinas, R. and Precht, W., editors, *Frog Neurobiology: A Handbook*, pages 33-77, Springer, New York, 1976.

[12] Purwaningsih, E. H., Ibrahim, N., & Zain, H. The nerve protection and in vivo therapeutic effect of Acalypha indica extract in frogs, *Medical Journal of Indonesia*, 19(2):96-102, 2010.

[13] Koles, Z. J. and Rasminsky, M. A computer simulation of conduction in demyelinated nerve fibers. *Journal of Physiology*, 227:351-364, 1972.

[14] Veit, S. and Struijk, J. J. Evaluation of the Cable Model for Electrical Stimulation of unmyelinated Nerve Fibers. *IEEE transaction on Biomedical Engineering*, 48(9):1027-1033, 2001

[15] Tai. C, Groat, W. C., and Roppolo, J. R. Simulation analysis of conduction block in unmyelinated axons induced by high-frequency biphasic electrical currents. *IEEE transaction on Biomedical Engineering*, 52(7):1323-1332, 2005.

[16] Quandt, F. N. and Davis, F. A. Action potential refractory period in axonal demyelination: a computer simulation. *Biological Cybernetics*, 67:545-552, 1992.

[17] Lowry, O. H., Rosenbrough, N. J., Farr, A. L., and Randall, R. J. Protein measurement with the Folin Phenol Reagent. *Journal of Biological Chemistry*, 193:265-275, 1951.

[18] Walker, J. Protein structure, purification, characterization and function analysis. In Wilson, K. and Walker, J., editors, *Principles and Techniques of Biochemistry and Molecular Biology*, pages 300-351, ISBN:978-0-521-51635-8. Cambridge University Press, Cambridge, 2010.

[19] Mukherjee, A. M. Correlation between the phospholipids domains of the target cell membrane and the extent of *Naja kaouthia* PLA2-induced membrane damage: Evidence of distinct catalytic and cytotoxic sites in PLA2 molecules. *Biochimica et Biophysica Acta*, 1770:187-195, 2007.

[20] Sekhar, C. C. and Chakrabarty, B. Fibrinogenolytic toxin from Indian monocled cobra (*Naja kaouthia*) venom. *Journal of Biosciences*, 36:355-361, 2011.

[21] Mukherjee. A. K. and Maity, C. R. Biochemical composition, lethality and pathophysiology of venom from two cobras - *Naja naja* and *N. kaouthia. Comparative Biochemistry and Physiology*, 131:125-132, 2002.

[22] Doley, R. and Mukherjee. A. K. Purification and characterization of an anticoagulant phospholipase A2 from Indian monocled cobra (*Naja kaouthia*) venom, *Toxicon*, 41:81-91, 2003.

[23] Katsuki, R., Fujita, T., Kogra, A., Liu, T., Nakatsuka, T., Nakashima, M., and Kumamota, E. Tramadol, but not its major metabolite (mono-O-demethyl tramadol) depresses compound action potentials in frog sciatic nerves. *British Journal of Pharmacology*, 149:319-327, 2006.

[24] Kini R. M. and Doley, R. Structure, function and evolution of three-finger toxins: Mini proteins with multiple targets. *Toxicon*, 56:855-867, 2010.

[25] Smith, L. A., Lafaye, P. J., LaPenotiere, H. F., Spain, T., and Dolly, J. O. Cloning and functional expression of dendrotoxin K from black mamba, a K+ channel blocker. *Biochemistry*, 32:5692-5697, 1993.